

A Graph-based Multi-modal Inter-subject Correlation Study For Naturalistic Viewing Paradigm

For Master of Science Thesis

by

Venkatesh SUBRAMANI

MSc in Data Science

IMT Atlantique

A dissertation submitted in partial fulfilment
of the requirements for the degree of
Master of Science

October 27, 2021

Keywords: EEG, Canonical Correlation Analysis, Inter-subject correlation, eLORETA, fMRI, Graph.

In accordance with the requirements of the degree of Master of Science in the , I present the following thesis entitled,

***A Graph-based Multi-modal Inter-subject Correlation Study For
Naturalistic Viewing Paradigm
For Master of Science Thesis***

This work was performed under the supervision of Nicolas FARRUGIA, Giulia LIOI. I declare that the work submitted in this thesis is my own, except as acknowledged in the text and footnotes, and has not been previously submitted for a degree at IMT Atlantique or any other institution.

Venkatesh SUBRAMANI

*If we knew what it was we were doing, it would not be called research,
would it? – Albert Einstein*

Acknowledgements

Abstract

Abbreviations

ISC - Inter-Subject Correlation

EEG - Electroencephalogram

fMRI - functional Magnetic Resonance Imaging

CCA - Canonical Correlation Analysis

MNE - Minimum Norm Estimate

eLORETA - exact Low Resolution brain Electromagnetic Tomography

DWI - Diffusion-Weighted Imaging

BEETL - Benchmarks for EEG Transfer Learning

EOG - Electro-Oculogram

PCA - Principal Component Analysis

BEM - Boundary Element Method

PSD - Power Spectral Density

RH - Right Hemisphere

SEM - Standard Error of the Mean

GSP - Graph Signal Processing

HBN - Healthy Brain Network **GFT**- Graph Fourier Transform

Contents

1 About the Host Institution	1
1.1 IMT Atlantique	1
1.2 MEE Department and Team BRAIn	1
2 Missions Undertaken	2
3 Rationale & Related Work	3
3.1 Research Question	3
3.2 Brief intro to Cognitive Neuroscience	4
3.3 Related work	5
4 Methods & Results	8
4.1 Dataset	8
4.2 Tools Handled	8
4.3 Pre-processing	9
4.4 Source Inversion	9
4.5 GSP	12
4.6 ISC	13
4.6.1 CCA	14
4.6.2 Graph	15
4.7 Results	16
5 Discussion	19
5.1 Summary of results & Discussion	19
5.2 Scientific Perspectives	21
5.3 Self-evaluation	21
5.4 Personal Reflections	22
A BEETL Challenge	24
Bibliography	28

Chapter 1

About the Host Institution

1.1 IMT Atlantique

Being part of the Institut Mines-Télécom group, a prestigious *grande école d'ingénieurs*, IMT Atlantique (IMTA) is producing high-throughput research in several technical disciplines such as Telecom, inter-disciplinary Artificial Intelligence, etc. After being named as IMTA, as a result of a merger between Mines Nantes et Télécom Bretagne, it turned multi-site spreading across three different campuses. Each year the graduating engineers are trained to not only assess the impact of their developed system on a narrow scale but encouraged to examine also the environmental, sociological side.

1.2 MEE Department and Team BRAIn

Mathematical and Electrical Engineering (MEE) department is involved both in pedagogy and research in the fields of data science, embedded circuits, digital communications, etc. Several research teams are part of the MEE, one such is Better Representations for Artificial INtelligence(BRAIn). The expertise of the team includes efficient, scalable AI most beneficial for the low-resource embedded systems, Cognitive Neuroscience, more generally Brain-Computer Interfaces, Graph Signal Processing, Few-shot learning, etc. Besides, the team participate in various competitions such as []. Collaboration with other universities such as Universite de Montreal is strongly pursued too. In addition to its AI research, BRAIn is also taking various measures on the Ethical front by conducting seminars where external invitees are welcomed.

Chapter 2

Missions Undertaken

You just keep pushing. You just keep pushing. I made every mistake that could be made. But I just kept pushing. — René Descartes

The missions range from working on the internship ISC project, participating in the BEETL challenge, to presenting research papers in Blitz. Each one of them has quirks hence dedicated efforts were necessary.

Let us start with the internship project; during the initial days of my stint, I was involved in examining what I brought & what I had, and with the help of my advisors, I analyzed the gap and the needed step to leap forward. Coming from an applied data science/Computer Science background, not only I had to get acquainted with Cognitive Neuroscience, but the clean transition to becoming a researcher was essential. To have a solid grasp on Cognitive Neuroscience, I happened to explore various resources such as reference-grade books[20, 39, 28], research articles[1], so forth. Once adequate competence was in place, analysis and manipulating the data to familiarize with the data structures began. The focus now shifted towards an extensive literature survey to learn the typical pipeline for a related project. The acquired knowledge helped me infer the results and enabled checking for the reliability of the results employing statistical significance.

Next, my involvement in the BEETL challenge— a huge chunk of the internship dedicated towards this deep learning-based competition where I happened to associate with other BRAIn team members ranging from Full-time professors, Post-docs, PhDs. Thanks to this competition, I got the opportunity to collaborate in a team environment that includes recurrent bi-weekly meetings, discussions, so forth. The specifics about this challenge are available in the dedicated appendix.

Concerning the engagement in the BRAIn-wide Blitz presentations, the goal here is to get informed with the ongoing research. There is a temporal constraint for the participants to meet— the duration of the presentation must be under 3 minutes. This pushes to look at the research articles differently, to pick the minimal right information yet preserving the core.

Chapter 3

Rationale & Related Work

“I was never aware of any other option but to question everything.” — Noam Chomsky

3.1 Research Question

How similar is the brain activity across subjects watching the same movie?



Figure 3.1: Base Image Credits[25], tweaks by author

Cinema takes viewers through a journey that evolves over time grabbing their attention and triggering perceptual, cognitive, and emotional

processes[25]. On the other hand, filmmakers have developed an ensemble of techniques such as gripping narration, elevating background score that complements storyline, to capture the viewers' attention. The recent developments of neuroimaging provide us with a way to capture the activity of the brain. This study primarily targets the sensory level physiological phenomena called Perception, where people watching the movie fondly called as subjects' brain activities are measured. For the sensory activities, the sensory inputs turn out to be a neuronal activity that leads to perception(bottom-up)[20]. The underlying principle behind a grander scale is Consciousness, in which the questions such as "What is consciousness & whether the science we know explains them" are debated. Perception is the input from the world to the mind, action is output from the mind-world while the thoughts are the mediating process[5]. Perceptions are through the stimulus from the environment to sense organs such as the eye, ear, or skin and are of several forms, such as visual, auditory, touch respectively. The definition of Inter-subject correlation, according to me, is the correlation of activity in the brain regions, or connectivity across subjects during some type of state – Resting-state or with a stimulus such as video-watching. There are ways to record the activity such as non-invasive neuroimaging which provides a peek into the living brain without cutting open. With the help of that, studies have uncovered that variability in humans is substantial[51]. For instance, the intra-subject fluctuations in resting connectivity between days were very different from the inter-subject variation[42, 50]. Understanding the richness of the naturalistic experimental paradigms enables us to investigate the social interactions[33].

3.2 Brief intro to Cognitive Neuroscience

The metabolically demanding human brain has roughly 100 billion neurons [8] and consumes 20% oxygen supply while its mass is only 2% of the body as there is no glucose reserve but to utilize real-time[20]. Glial cells estimated to be 1 trillion[8], support neurons in modulating electrical activity, so forth[20]. Neuroimaging helps measure the activity, and there are several widely known methods such as EEG, fMRI that measures electrical activity and the intensity of hydrogen molecules present in Blood respectively. Each one has its perks and pitfalls; for example, EEG is precise temporally (in ms) but spatially poorer compared to fMRI which is excellent (1-3 mm)[24] but temporally weaker (in 1-3s)[24]. EEG measures at the scalp level, and alternatively, magnetic-field-based fMRI non-invasively records at the deeper level. We used data from both these different modalities to have more accurate Spatio-temporal information available.

The brain is segregated into lobes, gyri that form lobes, sulci that connect gyri and lobes (see figure 3.2). Each one of them has a specific role associated. For instance, the occipital lobe is responsible for the Visual cortex; the Postcentral gyrus in the Parietal lobe is for somatosensory;

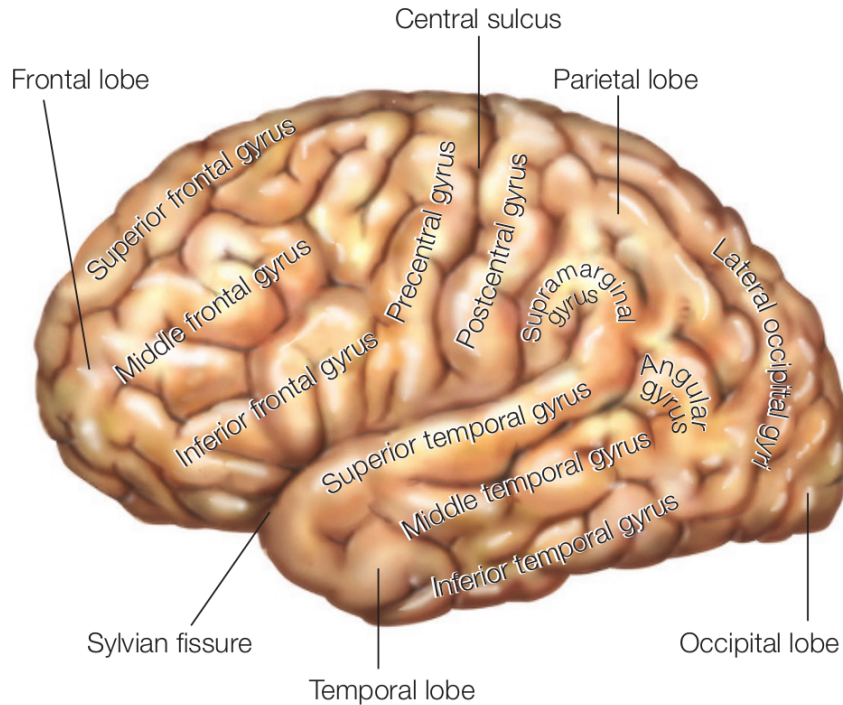


Figure 3.2: Anatomical brain. Image Credits[20]

the Precentral gyrus in the Frontal lobe is for the motor-cortex; Parts of the superior temporal gyrus in the temporal lobe is Auditory cortex[20]. The brain shares information between two cerebral hemispheres, besides, researchers have found evidence about the Lateralized brain – one side of the hemisphere dominates certain tasks and shares the information with the other side. This happens with the help of white matter, fiber tracts that connect two cerebral hemispheres through the Corpus callosum[20] chap 4]. The lateral cerebral cortex is considered to be a grey matter, and the way to represent them depends on the type of the measurement – Volumetric (MRI) or Surface (EEG). The parcellation methods spatially subdivide the brain based on homogeneity, for instance, homogeneous connectivity for connectivity-based parcellation[10]. With DWI, the connectivity graph is established using white matter, which could be attributed to the edges of a graph as it reflects some properties[44].

3.3 Related work

For decades most classical studies focus on the works conducted under a controlled environment with artificial stimuli, which changes recently to investigate the neural activity in more realistic conditions to under-

stand the brain under real-world sensory input[18, 29]. The study indicates that naturalistic viewing stimuli are increasingly used to engage cognitive and emotional processes during fMRI studies, however, EEG has been less employed to measure neural responses[12]. More specifically on the genre of movies, the suspense effect on the brain has been closely studied[49, 6, 37] which shed us light on – memory-related engagements when critical information appears[49], the positive correlation of pupil dilation with surprise[6], the usage of a highly engaging movie – Alfred Hitchcock’s ”You’re dead” – to determine the neural basis of executive processes common across individuals[37]. I am more intrigued by how does this translate into solving day-to-day problems such as treating behaviorally responsive non-responsive patients. The study from Naci et al.[37] outlines the ability to decode the conscious experience in such patients; Anil Seth in his book indicates that the standard clinical procedures to determining the conscious state of the brain-injured patient still rely on behavior such as the response to the sensory stimulation, to commands and so on[45].

This work from Dmochowski et al. analyses the ISC of the subjects during the naturalistic viewing (you’re dead) using just EEG, with the help of CCA on the scalp level to derive components and studies at the source space (vertices)[14]. The source inversion is done leveraging eLORETA and followed by the study of the effect of unscrambled scenes on the coherent brain signature. This paper also suggests the increased activity in theta band (4–8Hz) in frontal areas which is incorporated into memory encoding[14]. The authors of this paper state that the multimodal-based study in the future uses not only EEG but incorporating fMRI. However, to the best of my knowledge, there is no such study conducted by the same authors(Dmochowski et al). This paper[30], on the other hand, takes a different strategy to study the influence of attention on the ISC; the ISC analysis is deduced applying CCA but stays topographical without the source inversion, and concludes that the strong modulation of ISC was observed during the first attentive viewing as opposed to repeated viewing which diminishes the attention[30]

Graphs offer the ability to model complex data and its interactions among them[40], and despite the big strides in the recent decade, the understanding of the principles of the brain and its complex function remains incomplete[9]. The recent advancements in neural recordings enable not only does it make possible to get more precise information but recordings are large[9]. The aggregated data pose a challenge during statistical inference, even while dimensional reduction[13] for scalable computing[17], and so on. Bassett et al propose to leverage the use of Graphs, terming Network Neuroscience [9].

With regards to the studies on ISC leveraging graph, this study[44] follows a similar pipeline as this project such as multimodal datasets, source inversion, parcellation, followed by the analysis on the graph space with

the graph created using DWI. However, this is not an ISC-based study, alternatively, it uses simpler stimuli set up to compare the source space and the graph space in terms of measures such as effective dimensional reduction, signal compactness. In fact, to the best of my knowledge (duly validated with my advisors), studies have not yet been realized which follow the meaningful framework as this project does, and the latter targets to address the gap with the methodology– ISC-based study for the naturalistic stimuli on the graph space from source space using multimodal datasets.

Chapter 4

Methods & Results

4.1 Dataset

The philanthropy-funded HBN datasets are open-source, collected across several sites in the United States. Written consent was acquired from all the participants aged over 18 and from the guardians whose age is over 6 before the start of the experiment[31]. All the data are de-identified and consent was obtained to publicly share[31]. The measurements are for task-free resting state, task-based (video-watching), eye-tracking, taken from [] participants range between []. The experimental design varies based on the type of paradigm. For the resting state, the recorded voice instructed the subjects with ‘now close your eyes’(40s) and ‘now open your eyes’(20s), the duration of this paradigm is 350s. For the Naturalistic stimuli, video-watching on the other hand, the participants are instructed by ‘Now you can watch video clips. Enjoy! First, we have to measure the position of your eyes. Just follow with your eyes the circle. Press to begin.’. The duration of the video depends on the movie clip, the duration of the clip from ‘Despicable Me’ used for this project is 172s. The EEG is recorded using a 128-electrode channel array EEG geodesic hydrocel system with a reference at the vertex of the head (Cz)[38]. In this work, we considered 10 subjects whose average age is [] and ranges from []. The subjects are determined based on several criteria: the availability of the multimodal data, aged at least [] years to have a measurement from the matured skull, and hold a better signal-to-noise ratio[38].

4.2 Tools Handled

Open-source Python-based packages such as MNE[22] – for analysing, visualizing neurophysiological data, neuroquery[15] – a tool for meta-analysis for neuroimaging studies which queries publications, Nilearn[2] – a tool for statistical analysis for neuroimaging, Surfplot[19] – Brain Surface plots, PyGSP[], are used for this work among other conventional libraries.

4.3 Pre-processing

The HBN provides both preprocessed and raw data; in this work, we considered the former. Out of the 128 channels, 119 were used for scalp recording and 9 EOG were used for eye artifact removal. The electrodes placed in the outermost circumference (chin and neck) were also excluded[31]. The EEG data were high-pass filtered at 0.1 Hz, in addition to the eye artifacts were removed by linearly regressing the EOG channels from the scalp EEG channels[31]. Then, a robust PCA algorithm and Augmented Lagrange Multiplier Method (ALM) were applied to remove sparse noise from the data[31]. The ALM recovers a low-rank matrix A from the corrupted data matrix $D = A + E$ where E is noise/error[31]. Follow the suit is the visual inspection for each subject to discard the whole block and/or paradigm recordings that remained noisy after pursuing this removal methods[31]. Finally, the noisy channels are removed based on the extended pre-preprocessing methods [31] to become 91-channel array. The sampling of the provided data is at 500hz; in the view of reducing computational footprint, it was reduced to 250hz whenever deemed necessary.

4.4 Source Inversion

Source Inversion or Source Reconstruction on EEG data uses the measurement of differences in voltage potential across scalp and then uses the signal processing techniques to estimate the sources in the brain that fits best the measured data[23]. EEG does not directly measure the activity inside the neurons, instead, it picks up the signal coming from the post-synaptic potential where charges accumulate once the neurons make a connection at input synapses[20]. EEGs are recorded from the large population of neurons by the electrodes that are placed some distance away – scalp[20]. The geometry of the head and the presence of different types of tissues with various electrical conductive properties between cortex and scalp distort the signal, so it is not possible to associate sources to each electrodes[7]; also, there are as many sources as many neurons, it is also not plausible to capture single neuronal activity separately. The Source Reconstruction is an ill-posed inverse problem for which there is no unique solution, besides, it is highly sensitive to noisy data. Hence the stability depends on the forward and inverse modeling parameters[35]. Intuitively, forward modeling describes how the electric field spreads through the different layers of the head while taking the structural, conductive property of the tissues and geometry of the head into account.

Various implementations define these said properties. Freesurfer[16] is one of the open-source tools used in this project for forward modeling; it is a suite of powerful tools for neuroimaging that provides us the structural representation of the cerebral cortex[16]. The features include mapping of the thickness of cortical grey matter, inter-subject alignment of gyrus

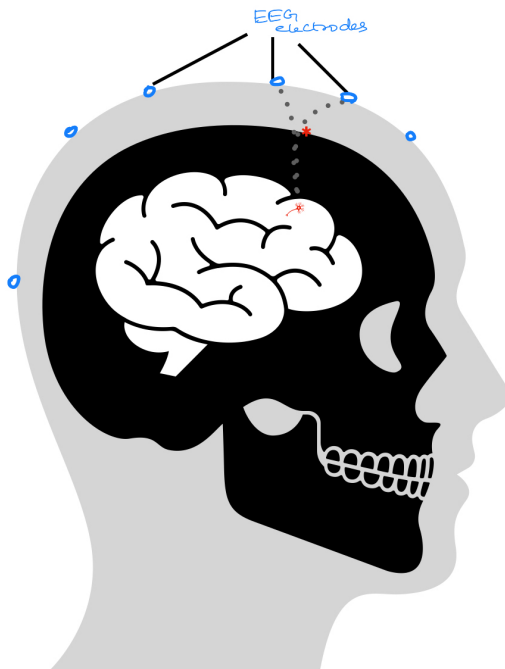


Figure 4.1: Anatomical brain. Image by Author

folding patterns[16]. More specifically, the **Freesurfer** **fsaverage** template is used to map the individual surfaces to a common coordinate system. The **fsaverage** version considered (version 5) for this project contains 10242 vertices on each hemisphere, which is observed to be the best compromise between accuracy and computational power & memory required.

BEM is used for the creation of realistic head modeling while factoring in different compartments of the head such as the scalp, thickness of the skull, and brain mesh generation[26, 4]. BEM is considered for this work as it was demonstrated to be accurate[4].

Finally, for the inverse operator, the noise covariance matrix for the electrodes is estimated. The noise can be of a different kind – biological, instrumental, and even ambient noise, that are present in the system. The objective is to distinguish the signal of interest from the noise which acts as a baseline. The said pipeline is presented in figure 4.2.

eLORETA is used in this work since it is well demonstrated to deliver zero localization bias in the presence of biological noise[47, 41]. The source that emerges from the lateral part of the brain is different from the ventral source; it is deeper thus leading to an increased possibility of attenuation,

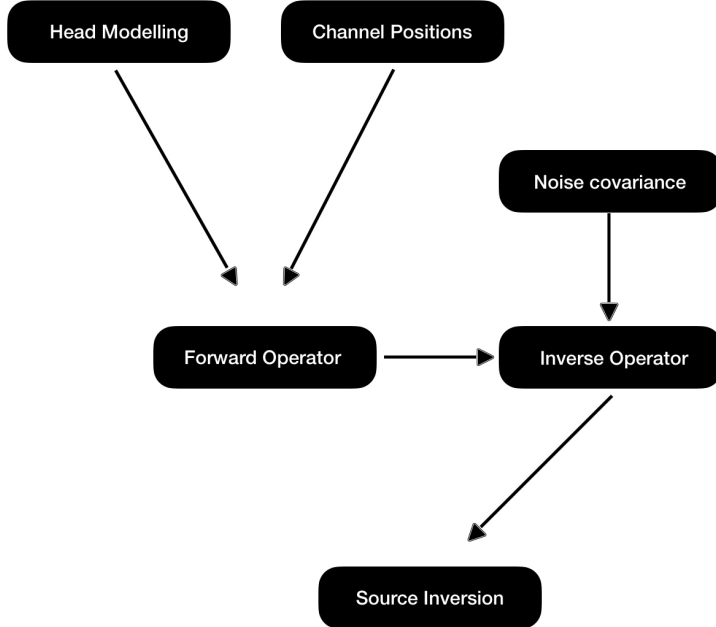


Figure 4.2: Pipeline for Source Inversion. Image by Author

mixing of signals, and so on. eLORETA, albeit being a linear inverse solution method, favors the deeper sources utilizing weighted norm for estimation.

As the source inversion is highly sensitive to noise and depends on the forward modeling, the reliability check of the established pipeline is indispensable. So, we decided to test the reliability measure by using the resting-state data. The resting-state from the HBN dataset contains two "events" – Eyes open, Eyes closed, which lasts 20s and 40s respectively. One subject is picked for this test case and the testing hypothesis is a well-established fact which reported in the 1930s – increased alpha activity during eyes-closed than eyes-open in the posterior region such as Occipital lobe[3].

Figure 4.3 illustrates the decreased alpha activity (8-13 Hz) during eyes-open from eyes-closed. The 95% confidence interval (CI) in the figure is entire vertices, and it is noticeably different among the two states. Not only is the mean across vertices for the eyes-closed higher than eyes-open, but also the CI is wider and higher. Next, to ensure whether this is statistically valid, a two-sample two-tailed t-test was applied, and the results

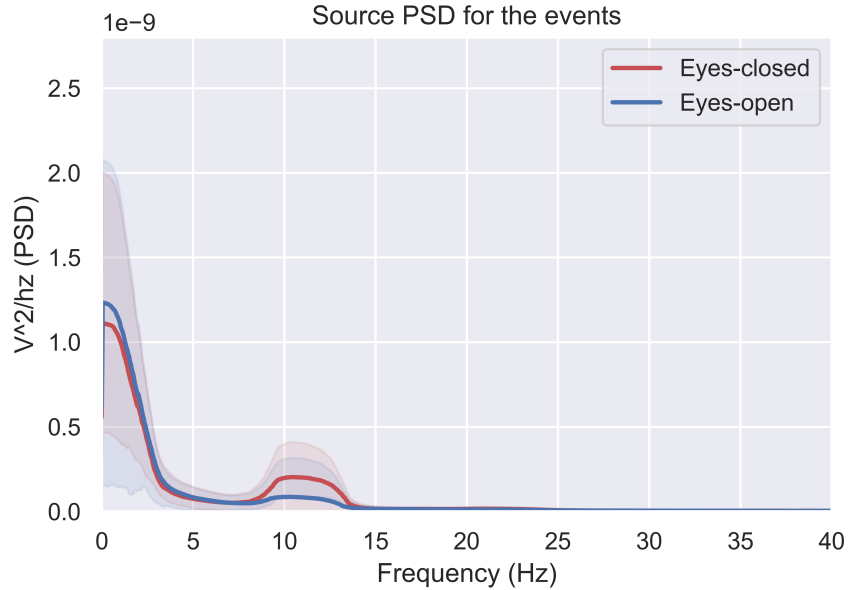


Figure 4.3: PSD at the source space

are as follows: p-value = 1.22e-63, t-value = 20.098. This implies the null hypothesis is rejected, and the t-value shows the mean power of the eyes-closed distribution is higher than that of eyes-open. With that, the stability of the source inversion is warranted.

4.5 GSP

Definition: A Graph g is a set of elements, such as nodes (vertices) and their connection between nodes (edges). More formally, $g = \{V, E\}$ where V and E represent vertices or nodes and E edges or links respectively. Let V_1, V_3 belongs V ; in a weighted network, the links have associated weights: (V_1, V_3, W) where W represents the weight between V_1, V_3 .

Degree Matrix, \mathbf{D} denotes the number of edges or neighbors associated with a node or vertex while the **Adjacency Matrix**, \mathbf{A} denotes the immediate neighbor of a node whose dimension is vertex \times vertex and a_{ij} is 1 when there is a neighbor between nodes i and j , 0 elsewhere. For instance, in figure .4, the degree for node 5 is 2 whereas node 5 has node 3 and node 4 as its neighbors.

Laplacian Matrix, \mathbf{L} explains the interaction and incidence in a network. It is denoted by, $\mathbf{L} = \mathbf{D} - \mathbf{A}$. **Eigenvector:** The basis vector(s) which remain(s) in its span after the linear transformation; the scaling of the remained vector is said to be **Eigenvalue**.

Structural Connectivity Graph: The contemporary neuroscience questions such as how does physical circuit affects its function, how does pathology spread through cortical and subcortical tissue, have given rise

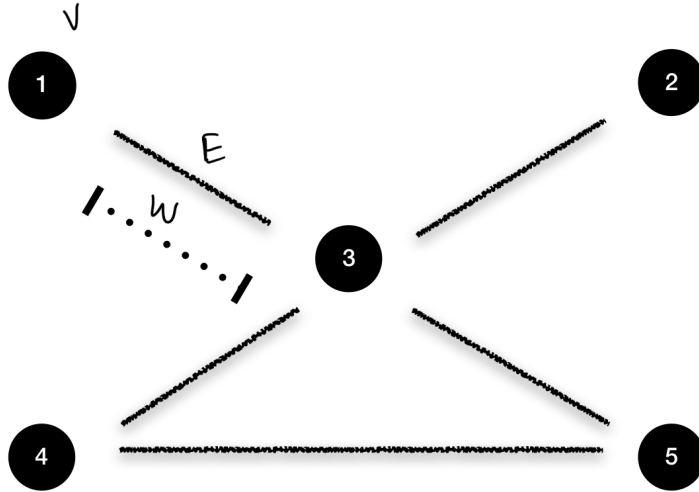


Figure 4.4: An undirected weighted Graph. Image by Author

to investigate the anatomical, connectivity of the brain[46]. One of the whole-brain imaging techniques, DWI reveals the underlying white-matter pathways[43]. In this work we used the data provided by the Human Connectome Project(HCP)[48], which studied 56 healthy volunteers using DWI. Followed by the analysis on DWI scanning, it used the glasser parcellation cortical atlas[21] which consists of 180 parcels (ROIs) at each hemisphere to average the regions structurally[43]. Specific details are available in the glossary.

Graph Fourier Transform is the spectral decomposition of a (brain) signal based on the topology. More formally, L can be decomposed into eigenmodes such as eigen values and eigen vectors – $L = U$ (crescent) U^T , then, $GFT = U^T \text{Signal}_{\text{brain}}$. GFT provides the spectral information of the brain signals on the graph; it is used to exploit the graph frequency bands to interpret the data[34]. The low frequency bands correspond to more localized connectivity whereas the high frequency bands characterize “noisy” signature (see figure 1D in[34]).

4.6 ISC

We studied how (dis)similar the neural responses are when the healthy young adult subjects are exposed to the same movie clip. The analysis is two-fold: first, CCA is applied at the scalp level to find the correlation at the measured signal, followed by the analysis on the source space; second,

parcellation has been applied on the source space signal followed by its analysis on the graph space with the structural connectivity graph.

4.6.1 CCA

PCA and CCA possess similar properties except, the PCA maximizes variance while the CCA maximizes correlation. Given the multi-channel multi-subject data, CCA finds the weights such that the subject vectors exhibit maximal correlation. Concretely, let us consider, for instance, the CCA for 2 subjects[14]:

$$\hat{\omega} = \arg \max_{\omega} \frac{y_1^T y_2}{\|y_1\| \|y_2\|} \quad (4.1)$$

\mathbf{w} weight matrix $\in \mathbb{R}^{1 \times C}$, $y_1, y_2 \in \mathbb{R}^{C \times T}$ where C is channels and T is time samples.

$$\hat{\omega} = \arg \max_{\omega} \frac{\omega^T R_{12} \omega}{\sqrt{\omega^T R_{11} \omega} \sqrt{\omega^T R_{22} \omega}} \quad (4.2)$$

\mathbf{R}_{ij} represents covariance matrix between subjects i, j $\in \{1, 2\}$.

Differentiating on equation 4.2 with respect to w provides:

$$\frac{\sigma_{11}\sigma_{22}}{\sigma_{12}} R_{12} w = (\sigma_{22}R_{11} + \sigma_{11}R_{22}) w, \text{ where } \sigma_{ij} = w^T R_{ij} w \quad (4.3)$$

$$(R_{11} + R_{22})^{-1} (R_{12} + R_{21}) w = \lambda w \quad (4.4)$$

where $\lambda = \sigma_{12}/\sigma_{11}$. The spatial filter that maximizes correlation follows the eigenvector of $(R_{11}+R_{22})^{-1} (R_{12}+R_{21})$, where its eigenvalues explain the correlation coefficient. Solving linearly with the spatial weight vector \mathbf{w} , data covariance matrix \mathbf{R} provides the components $\in \mathbb{R}^{C \times T}$.

Implementation: The 91 components are obtained after applying CCA to the data. We chose first three components which summarizes the correlation the best[11, 27]. Then, as a stringent measure, we implemented bootstrapping to establish a noise floor. More precisely, the 172s time-series is divided into 5-s window blocks, then the blocks are randomly shuffled to create a new ISC coefficient time-series, this is run for 1000 times (see figure 4.5). The coefficients are significant for approximately 12% (21s) of the whole duration (172s).

Subsequently, the "High ISC" and "Low ISC" periods are picked. The period where the coefficients are close to zero is considered as Low ISC. 1-second of data are chosen for the two conditions in this format: ± 0.5 s from the period – the High ISC tops at 159th second, so the chosen data is between 158.5 and 159.5 seconds.

Source Inversion is done for all the 10 subjects independently to preserve the intricate event-related potentials which would be missed if averaged over subjects. Source Inversion is memory-intensive, especially

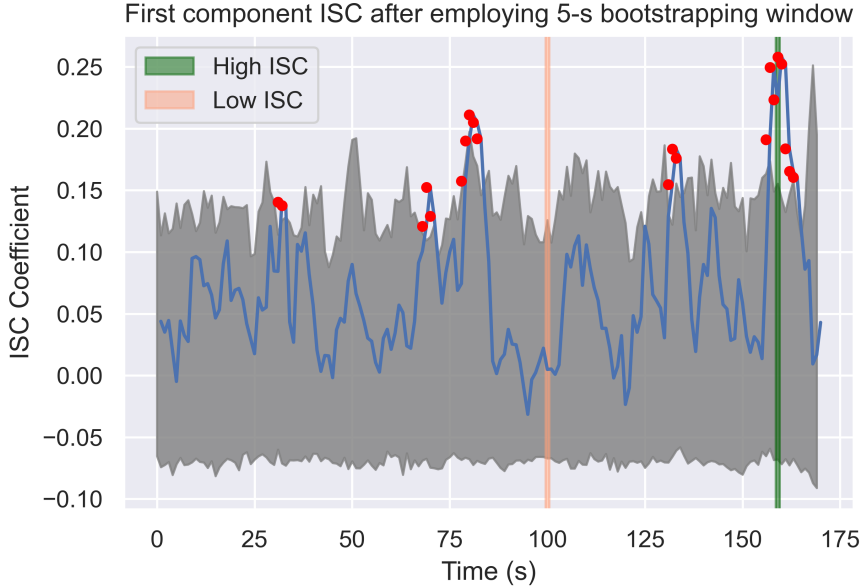


Figure 4.5: Significance of ISC coefficients following the noise floor

the estimation of the covariance matrix, therefore inverting the entire 172s data is ignored. Instead, we took the data from the two conditions – High and Low ISC (see figure 4.5). As part of the source inversion, the inverse operator requires a noise baseline at the electrode space; we picked the data from a task-free state and regularization has been applied. Once the source inversion is done, the statistical reliability has been promptly validated after parcellating – one-sample t-test is applied on high - low activation data besides the t-test on Pearson correlation coefficients.

4.6.2 Graph

The parcellation has been carried out using Glasser et al. methods, which averages the vertices that are functionally homogeneous[21]; the eLORETA activations after applying parcellation is henceforth called as source space signal. Meanwhile, the graph which contains 360 nodes and edges based on the structural connectivity[43], is made ready, besides, *combinatorial* laplacian type is used to establish a graph.

The Fourier basis, which decomposes the graph laplacian into eigenmodes (eigenvector, eigenvalues), is computed; it is followed by applying GFT on the source space signal to obtain the spectral information. The GFT is done independently on Low and High ISC, likewise for each subject. Next, the spectrogram is computed by averaging through the subject dimension, likewise the standard deviation to assess the frequency or time that appears to be an impacting factor.

In addition, the graph PSD time-series is computed; to see the perti-

nent power spikes appropriately reflect the neural activations, we not only divided the graph spectrum into two parts – Low and High frequencies but it is divided such that the power distribution is the same. Further, the indicator function is used to filter the frequencies-of-interest after applying the l_2 norm on top; mathematically[44],

$$P_L^t = \left\| \mathbf{1}_{[\lambda < \lambda_{T.}]} U^\top s^t(r) \right\|_2 \quad (4.5)$$

$$P_H^t = \left\| \mathbf{1}_{[\lambda \geq \lambda_{T.}]} U^\top s^t(r) \right\|_2 \quad (4.6)$$

where λ represents Eigen values, U being Eigenvector and $s^t(r)$ is the source space signal.

Subsequently, the graph PSD as a function of eigenvalues is analyzed for both the conditions – High and Low ISC, and the subjects being the confidence interval besides averaging temporally; this gives insights into the frequency-wise subjective variability pattern in both conditions.

After a few iterations of observation, we identified that there is a presence of high fluctuations, notably in the specific frequency range, which made us consider smoothing besides using SEM instead of 95% confidence interval. Upon doing so, the frequency spectrum is trichotomized where low represents frequency 2 through 52, 52 through 200 for medium, and 200 through 360 for High; we discarded frequency 1 as the first eigenvalue, eigenvector pair is essentially 0. Afterward, the statistical validation is performed using one-way ANOVA between three groups and a t-test between Low versus High ISC for three frequency groups individually.

Following the observation on the spectrogram, we ascertained that frequency 7, in the eigenmode – eigenvector 7, explains the activations for the high ISC; then the corresponding eigenvector is visualized in the brain surface.

4.7 Results

I would never die for my beliefs because I might be wrong – Bertrand Russell

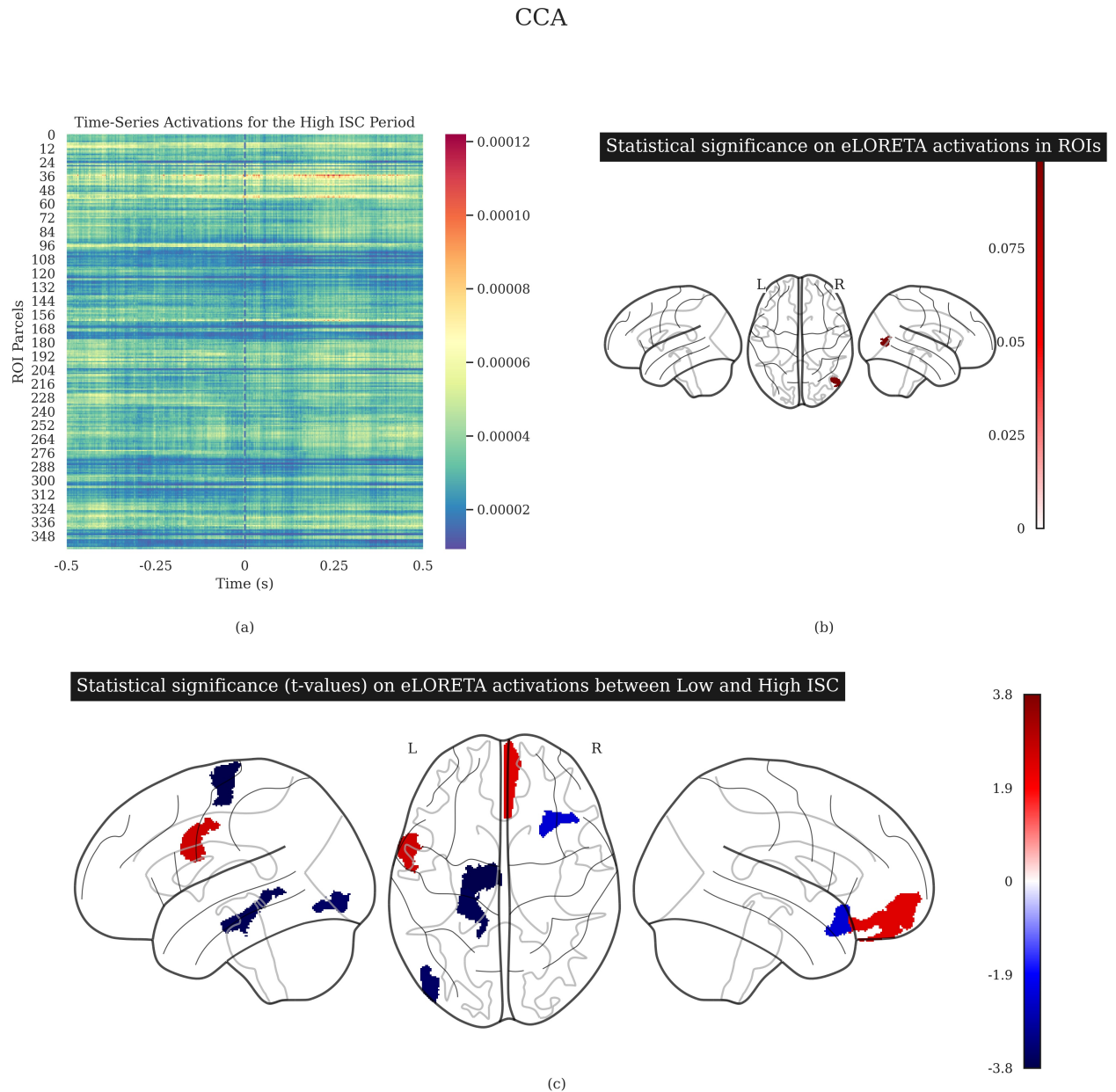


Figure 4.6: **a)** Time-series activation during the High ISC period averaged through subjects. **b)** The Region(ROI) where the statistical significance ($p < 0.0001$) is observed on the eLORETA activation data after differencing Low ISC from High ISC (high - low) – it is encoded with 1 if significant and 0 otherwise. **c)** Pearson Correlation Coefficient test is applied on the eLORETA activations, followed by the statistical significance test on it, $p < 0.05$.

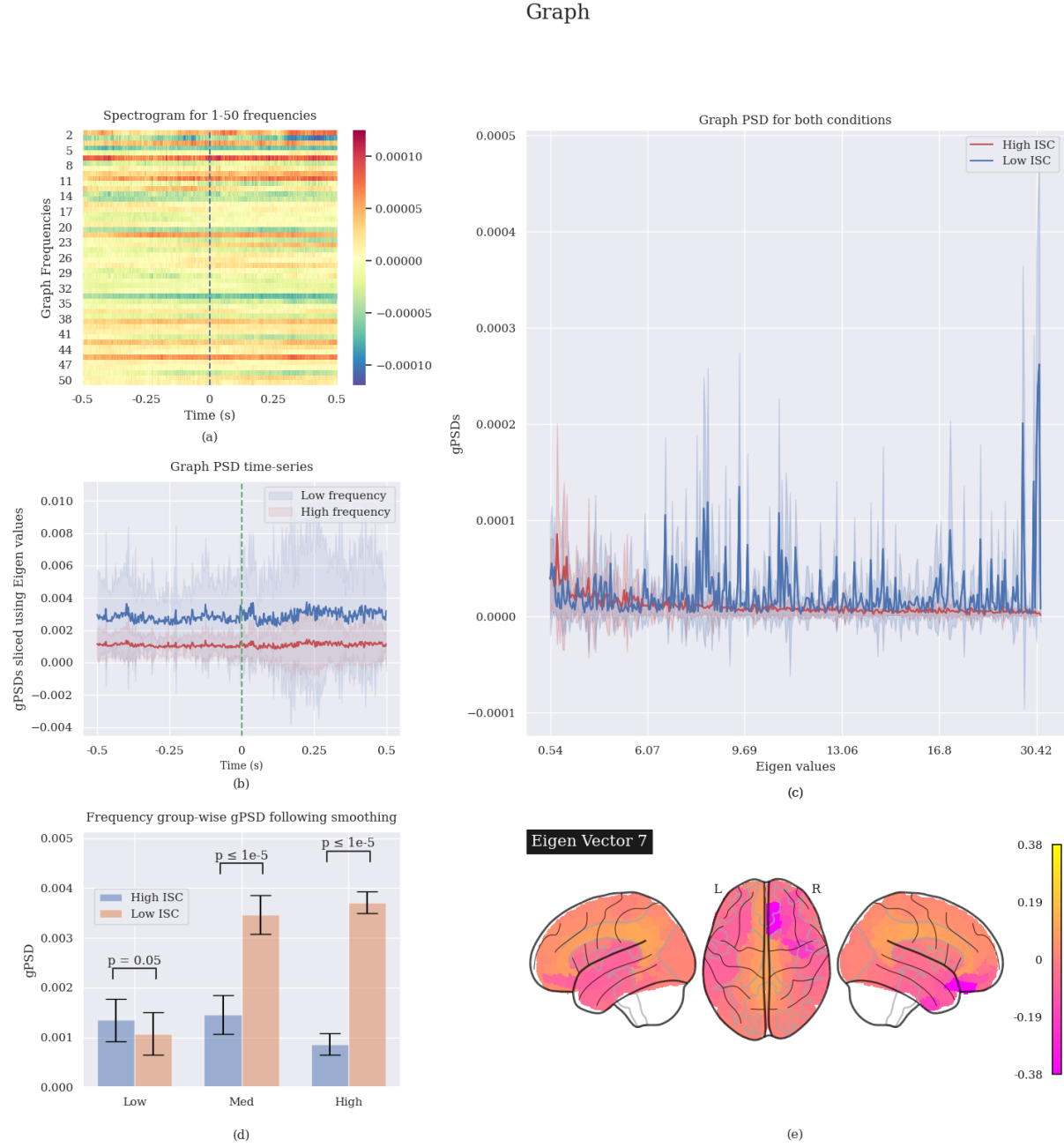


Figure 4.7: **a)** Spectrogram time-series for the low frequencies averaged across subjects. **b)** Graph PSD time-series for High ISC while the confidence interval being subjects. **c)** Graph PSD for the said conditions after averaging across time and the confidence interval is subjects dimension. **d)** Averaged Graph PSDs with smoothing after trichotomizing the frequencies and the error bars represent Standard Error from population mean. **d)** The seventh Eigen vector of structural graph on the brain surface.

Chapter 5

Discussion

5.1 Summary of results & Discussion

As depicted in figure 4.5, the ISC coefficients are close to zero most of the time – around 76% of the 170s the coefficients are below 0.10; two peaks can be observed – 80th second and 159th second, of which, the latter is very robust. We watched the video to identify what phenomena carry out these peaks; briefly, the video[] is about a father reading a bedtime story to his adopted daughters upon their requests; the bedtime story is about putting children which involves a mother. The father starts narrating and the kids start falling asleep slowly, around the 159th second once the reading is over, he gives a pause for a few seconds, no words uttered, while the mild background music is dominant, and then suddenly he scales up the tone and increases the volume, that is the period where the CCA tops.

Once the Low and High ISC periods are determined, eLORETA is invoked for source inversion, which is done independently for the said periods and also subject-wise. Figure 4.6a demonstrates the time-series eLORETA activations averaged through the subject, which can be interpreted in two dimensions – Space (ROIs) and Time (Seconds). The spatial significance is well pronounced, notice in the ROIs such as around 36 and 50, the eLORETA activation is higher whereas in the temporal front, the significance is pronounced between 0s and 0.25s in the said ROIs. Given the fact that the entire 1s window near 159th is already a high ISC period (see figure 4.5), the temporal insignificance is understandable. Concisely, the specified ROIs are observable during the specific period for all the subjects. However, averaging through subjects fail to capture very subtle variations, so to find the true statistical variations between High and Low ISC periods, we conducted a one-sample t-test for each of 360 ROI regions separately after differencing the pairs instead of a two-sample paired t-test for which the statistical significance is always true as it finds the variations between the mean on paired difference and the population mean. The results can be

seen in figure 4.6b which demonstrates the ROIs where there is a statistical significance ($p < 0.0001$). There are 4 significant ROIs – [0, 4, 6, 22] – for which the t-values are – [0, 9.52e-278, 8.89e-079, 9.97e-002]. Considering the scale of the eLORETA activations, only the ROI 22 – Visual Cortex RH, whose t-value is 9.97e-002, appears to be significant while the remaining suggests there is no difference. This result suggests that except for the one ROI, activation intensity between Low and High ISC is equal, which is misleading and made to question the randomness in the eLORETA system.

We proceeded with ensuring the reliability of the eLORETA system, likewise finding the presence of correlation after applying source inversion. For that the Pearson Correlation has been used; on the source space, the intra-person correlation is applied on Low and High ISC data individually for each ROI region. On the obtained result, which is in subject x subject dimension, the two-sample t-test is performed and the results can be seen in figure 4.7a. This t-test reveals there are 6 ROIs that are statistically significant. Considering how the t-test has been carried out, it reveals that in two of the significant ROIs, there is a presence of positive t-values, which therefore indicates the correlation for High ISC is higher than during Low ISC.

Once the statistical validity is analyzed, the transition to the Graph space is initiated with the estimation of PSD for the source space signal. Figure 4.7a represents the spectrogram for the time series after differencing the power between High ISC and Low ISC's data; therefore the positive value indicates the power in High ISC is higher than Low ISC's. This further suggests that the frequencies at which the differenced power is greater than zero could be responsible for neural activations. Higher power is observed in the frequencies until 13, where the concentration of frequencies that have higher power is more. Also, there are some intermediate frequencies between 22 and 35 that have sub-zero power followed by the frequency 46 where there is a presence of power above zero. Based on the spectrogram, it is quite clear that it cannot be categorically concluded that low frequencies are accountable for the activation.

Then, graph PSD time-series is estimated (see figure 4.7b)) to be able to see the power spikes given temporal dimension. Since the confidence interval is a subject dimension, it is possible to gain insights into the subject variability. As expected, and supported by figure 4.7b, the temporal dimension is invariant, as the whole duration of 1s is already in the High or Low ISC zone, it is not strictly possible to see the spike just at 0s (see figure 4.7b). Upon inferring this figure, there is a large subjective variability low frequency compared to high frequency while their averaged power for low frequency is higher than high frequency. Besides, between 0 and 0.25s, the confidence interval for both frequencies is relatively wider than during another period.

Upon learning the temporal insignificance, we then averaged temporally to create a graph PSD but as a function of eigenvalues while keeping the

subject as the 95% confidence interval (see figure 4.7c). In this figure, it is noticeable that both the confidence window, its mean power for High ISC is substantially narrower and lesser respectively than Low ISC, and its power is closer to zero beyond eigenvalue 6. Furthermore, in the initial eigenvalues range, however, a different trend is observed – the confidence window is wider which indicates that the power across subjects is not similar and the variation is present.

In the view of discovering the subjective variability appropriately, we attempted to use SEM which explains the variations from the overall population meanwhile considering the number of observations (see figure 4.7d) and it is represented through error bars. The SEM exhibits the variation across Low and Medium frequencies for Low and High ISC is the same while appears to be a reduction in the High frequencies. Applying one-way ANOVA between the frequency groups discloses the statistical significance with p-value = 0.0008 and f-value = 7.14; likewise, the student t-test between the conditions in each group separately (see figure 4.7d) which reveals the presence of comfortable significance in medium and high frequencies and the low frequency, however, the p-value is very close to the imposed threshold, the reason could be hypothesized as the low statistical power in these data. Besides, among these groups, the t-values indicate that the mean of the High ISC is higher than its counterpart in the low frequency and the opposite trend is evident in the remaining group.

The careful inspection at spectrogram paved the way to visualize the seventh eigenvector on the brain surface which then demonstrates the negative rightTermToFill across the ventral segments in both hemispheres..

Discussion:

5.2 Scientific Perspectives

5.3 Self-evaluation

“Knowing how to think empowers you far beyond those who know only what to think.” – Neil DeGrasse Tyson

Getting what was hoped (sometimes or most often) requires perseverance, resilience alongside. Metaphorically, where I am now is influenced by what I did yesterday. Thanks to the self-introspection I carry every now-and-then and the world I perceive psychologically, it is much easier to compare myself how I was before the internship versus how I am right now. I am glad that I can see the significant difference in a span of 6 months or so.

How I used to be: Even though I was measurably willing to go out of the comfort zone, how far I would cross would have been restrained by other factors. I would think deliberately logically before addressing, but surely I would not go much deeper to convince me. I would unhesitatingly

claim that, at IMT, more than Data Science & Engineering, I have learnt how to think and learn anything, which came in handy all the time.

What was demanded to conduct Research: The situation demanded me to grasp two things: Neuroscience, entirely new field than I was exposed to, academically and the second is Research. I would say the former can be pedagogically acquired whereas the latter is not a learnt skill but a practiced one. I had to relearn the day-to-day things such as how to effectively use the available resources to get a result, make an inference, validate, pick thenceforth a thread leads to a new potential path, and repeat.

How I approached to adapt: The above-mentioned things used to run on my mind often. Whenever I came across anything that I feel would help me has been directed to my advisors, who offered in return their wisdom. Once grasped, I mixed them with my experience and that I can stretch, and then it is duly applied in daily life.

5.4 Personal Reflections

I know that I exist; the question is, What is this 'I' that 'I' know.

I think; therefore I am. – René Descartes

Neuroscience: Questioning, especially me, has shed bright light that I cannot even quantify its luminosity. I think if not for this book[36], my venturing to Neuroscience would have been delayed for sure, if not never. I reckon no knowledge is lost; from my personal experience, knowledge, if handled skillfully, would support autonomously when the situation necessitates, then the only role is to listen. It makes me embrace the influence of Know-How on the knack of decoding puzzles. Neuroscience is one of the frontiers that has been investigated inadequately, and doing so would educate immensely. It matches my standards perfectly. Soon after starting this internship, neuroscience has left me to question everything on a hugely broader scale. For example, before the exposure to neuroscience, in my prime form, I would just have stretched deep to understand from the fundamentals; these days, however, I would go deeper – the scale from deep to deeper is larger than going until the visible horizon, that opens up a vast arena.

Consciousness: The above-mentioned quote says everything about how I think. This is surely a by-product of the navigation to wider arena. The simplest question I can think of, for which known science offers no answer – What makes Venkatesh Venkatesh, where do I have to draw boundary between Venkatesh and the person inside that I do not know. This is a classical question, termed Mind-body problem.

Psychology: Everyone is vastly different; it is impossible to *precisely* know how a person would think & act. I would not even attempt to

say that I completely know how I would react in a given situation. It intrigues me to view and consider Psychology without bringing "I" into any problem.

Appendix A

BEETL Challenge

A graph-based data augmentation strategy to integrate different Motor Imagery datasets and improve transfer learning

Venkatesh SUBRAMANI^a, Myriam BONTONOU, Ghaith BOUALLEGUE,
Nicolas FARRUGIA, Giulia LIOI

a: firstname.lastname@imt-atlantique.net, firstname.lastname@imt-atlantique.fr

IMT Atlantique, Lab-STICC, UMR CNRS 6285, F-29238, France

October 11, 2021

1 Introduction

The purpose of the motor imagery decoding task is to learn to classify 3 classes (left hand, right hand, other) from a small number of training examples (140 per class). In this challenge, the class *other* gathers two subclasses (feet and rest). As it is difficult to train a decoder from few data, the BEETL Challenge provides more data, called source data, to pretrain the decoder.

Tables 1 and 2 in appendix detail the data format of the three source datasets and of the two target datasets. The target dataset contains the training examples of the task of interest, while the source dataset is based on three studies containing examples of diverse classes.

Several challenges are raised by the transfer from the source datasets to the target dataset:

1. Classes are unbalanced (left hand and right hand are more represented than the others classes).
2. Transfer across subjects is known to be difficult due to inter-subject variability.
3. Different protocols are used to collect data across studies. The data format varies in terms of number of electrodes, position of the electrodes, sampling rate and filtering strategy.

In the Methods section, we explain how we addressed these challenges.

2 Methods

Our strategy consisted in pre-training a deep neural network (DNN) on all the source datasets and then, in fine tuning the last layers on the examples of the target dataset using an adaptive fine-tuning strategy.

2.1 Adapting the Input Data: Standardization and Data Augmentation

To address the challenge raised by the various data format, we first tried a naive approach and standardized all data samples to the same format. In particular we considered a subset of 17 electrodes¹ common to all datasets and resampled all examples to the same sampling frequency. However, this method had two obvious limitations. First, it required to know the format of the target dataset. Then, it amounted to set aside a huge amount of information.

We wanted to train a DNN with the same input shape for all datasets. In the following, more elaborate approaches are presented to handle missing electrodes and varying recording duration.

2.1.1 Graph-based interpolation of missing electrodes

In order to keep the maximum spatial (i.e. electrodes) information, we considered all the electrodes available across datasets, and performed a graph-based interpolation of the electrodes missing in the different datasets. The primary idea is to find the spatial neighboring electrodes for each of the missing electrodes. We used neighbors_graph² to spatially (distance-based) find the neighbors by creating the edges, and adapted it in such a way that for all missing electrodes at least two neighboring electrodes existed. We then performed an average of top two neighboring electrodes signals to create a new one.

¹[C1, C2, C3, C4, C5, C6, CP1, CP2, CP3, CP4, CPz, FC1, FC2, Fz, P1, P2, Pz]

²Sklearn

2.1.2 Varying the time window onset

Two issues are raised by the temporal dimension of signals. First, the data samples contain recordings over 3 or 4s but we believe that the activity linked to the motor task concerns a shorter time window. Second, the duration of the recordings varies across the datasets.

To circumvent these issues, we propose to train a DNN on a portion of the time series containing a fixed number of components by randomly selecting a portion of the time series. For instance, with a sampling rate of 160 Hz, we select a portion containing 445 time points (about 2.8 s). As such, the DNN is less likely to focus on the onset of the signals to classify them. Note that we choose to train the DNN on a relatively large portion of the data to avoid to remove the signal of interest.

2.2 Models and Hyperparameters Search

We tried several architectures of DNN, known to be efficient for motor imagery decoding. We first trained them to recognize the classes contained in the source datasets. Using the Weights and Biases platform <https://wandb.ai/site>, we tested many hyperparameters linked to the DNN architecture (e.g. number of layers) to the optimization of the training process (e.g. Adam or SGD optimizer, learning rate scheduling), to the data format (e.g. sampling rate, size of the temporal window, minimal and maximal frequency). We finally ended up with a Deep4Net model.

2.3 Adaptive fine tuning strategy

We adapted the last layer of the pre-trained Deep4Net [REF] to classify the target classes. Along with the training of this last layer on the new data, the layers of the DNN can be fine-tuned (i.e. trained on the new classes). As it is sometimes more efficient to fine-tune only the last layers of the DNN, we set the number of layers to fine-tune as an hyperparameter, as in the adaptive fine-tuning paradigm proposed by Zhang et al [1]. With this transfer strategy, the pre-trained DNN learns to extract data features which are of interest for classifying the source classes. We hope that these features will be also relevant for the new target dataset.

3 Results

About the pretrained DNN on the source datasets, we split the source data into a train and a validation set to estimate the ability of the DNN to generalize to new samples. We noticed that the performance on the validation set is consistently 55% irrespective of the hyperparameters. Besides, the choice of optimizer played the most significant role in our modeling process. So while modeling with the hyperparameter grid search, we have obtained both overfitting and underfitting on the same model.

4 Discussion

The variability between subjects is substantial. Besides, there are several challenges that we cannot skip ahead. For example, heterogeneity on the EEG amplifier, the impact of electrode placement due to the inconsistency at the subjects' head shape. We handle them with the techniques such as varying temporal window, interpolation of missing channels, careful model selection, etc. Despite introducing them, the improvement on the validation set is not visibly boosted, likewise on the leaderboard set. We suspect this is because of the bias in the model, which learns only the easiest examples and leans on them, so it struggles to differentiate specific classes. Also, the usage of the class *other*, which contains several classes, plays a noticeable role in the capability of the model. The diversity between left, right hand, and 'others' is substantial, some of the early-stage models were visibly biased towards either set of the classes.

5 References

1. Zhang, Kaishuo Robinson, Neethu Lee, Seong-Whan Guan, Cuntai. (2020). Adaptive transfer learning for EEG motor imagery classification with deep Convolutional Neural Network. *Neural Networks*. 136. 10.1016/j.neunet.2020.12.013.

Table 1: Description of the 3 source datasets and of the 2 target datasets. LH stands for left hand, RH for right hand, H for both hands, F for feet, T for tongue and R for rest.

	SOURCE			TARGET		
	Name	Cho2017	PhysionetMI	BNCI2014001	Leaderboard A	Leaderboard B
Classes	LH, RH	LH, RH, H, F	LH, RH, F, T	LH, RH, F, R	LH, RH, F, R	LH, RH, F, R
Number of examples per class	LH: 4940 RH: 4940	LH: 2480 RH: 2438 H: 2465 F: 2455	LH: 1296 RH: 1296 F: 1296 T: 1296	LH: 50 RH: 50 F: 50 R: 50	LH:90 RH:90 F:90 R:90	

Table 2: Format of the data in the 5 datasets.

	SOURCE			TARGET		
	Name	Cho2017	PhysionetMI	BNCI2014001	Leaderboard A	Leaderboard B
Number of electrodes	64	64	22	63	32	
Sampling rate (Hz)	512	160	250	500	200	
Duration (s)	3	3	4	4	4	

Bibliography

- [1] The networked brain - <https://cognitionemotion.wordpress.com/2021/02/20/the-brain-network/>, Feb 2021. 2
- [2] A. Abraham, F. Pedregosa, M. Eickenberg, P. Gervais, A. Mueller, J. Kossaifi, A. Gramfort, B. Thirion, and G. Varoquaux. Machine learning for neuroimaging with scikit-learn. *Frontiers in Neuroinformatics*, 8, 2014. 8
- [3] E. D. Adrian and B. H. C. Matthews. The berger rhythm: Potential changes from the occipital lobes in man. *Brain*, 57(4):355–385, 1934. 11
- [4] Z. Akalin-Acar and N. G. Gençer. An advanced boundary element method (bem) implementation for the forward problem of electromagnetic source imaging. *Physics in Medicine and Biology*, 49(21):5011–5028, 2004. 10
- [5] N. Alva. *Action in perception*. MIT Press, 2006. 4
- [6] J. W. Antony, T. H. Hartshorne, K. Pomeroy, T. M. Gureckis, U. Hasson, S. D. Mcdougle, and K. A. Norman. Behavioral, physiological, and neural signatures of surprise during naturalistic sports viewing. *Neuron*, 109(2), 2021. 6
- [7] A. Anzolin, P. Presti, F. V. D. Steen, L. Astolfi, S. Haufe, and D. Marinazzo. Effect of head volume conduction on directed connectivity estimated between reconstructed eeg sources. 2018. 9
- [8] C. S. V. Bartheld, J. Bahney, and S. Herculano-Houzel. The search for true numbers of neurons and glial cells in the human brain: A review of 150 years of cell counting. *Journal of Comparative Neurology*, 524(18):3865–3895, 2016. 4
- [9] D. S. Bassett and O. Sporns. Network neuroscience. *Nature Neuroscience*, 20(3):353–364, 2017. 6
- [10] E. Bonmati, A. Bardera, and I. Boada. Brain parcellation based on information theory. *Computer Methods and Programs in Biomedicine*, 151:203–212, 2017. 5
- [11] R. Bro and A. K. Smilde. Principal component analysis. *Anal. Methods*, 6(9):2812–2831, 2014. 14

- [12] W.-T. Chang, I. P. Jääskeläinen, J. W. Belliveau, S. Huang, A.-Y. Hung, S. Rossi, and J. Ahveninen. Combined meg and eeg show reliable patterns of electromagnetic brain activity during natural viewing. *NeuroImage*, 114:49–56, 2015. [6](#)
- [13] J. P. Cunningham and B. M. Yu. Dimensionality reduction for large-scale neural recordings. *Nature Neuroscience*, 17(11):1500–1509, 2014. [6](#)
- [14] J. P. Dmochowski, P. Sajda, J. Dias, and L. C. Parra. Correlated components of ongoing eeg point to emotionally laden attention – a possible marker of engagement? *Frontiers in Human Neuroscience*, 6, 2012. [6](#), [14](#)
- [15] J. Dockès, R. A. Poldrack, R. Primet, H. Gözükan, T. Yarkoni, F. Suchanek, B. Thirion, and G. Varoquaux. Neuroquery, comprehensive meta-analysis of human brain mapping. *Elife*, 9:e53385, 2020. [8](#)
- [16] B. Fischl. Freesurfer. *NeuroImage*, 62(2):774–781, 2012. [9](#), [10](#)
- [17] J. Freeman, N. Vladimirov, T. Kawashima, Y. Mu, N. J. Sofroniew, D. V. Bennett, J. Rosen, C.-T. Yang, L. L. Looger, M. B. Ahrens, and et al. Mapping brain activity at scale with cluster computing. *Nature Methods*, 11(9):941–950, 2014. [6](#)
- [18] A. Gait, V. Duisenbinov, M.-H. Lee, F. Biesmann, and S. Fazli. Inter-subject correlations during natural viewing: A filter-bank approach. *2020 42nd Annual International Conference of the IEEE Engineering in Medicine and Biology Society (EMBC)*, 2020. [6](#)
- [19] D. J. Gale, R. Vos de Wael., O. Benkarim, and B. Bernhardt. Surfplot: Publication-ready brain surface figures, Oct 2021. [8](#)
- [20] M. S. Gazzaniga, R. B. Ivry, and G. R. Mangun. *Cognitive neuroscience: the biology of the mind*. W.W. Norton Company, 2019. [2](#), [4](#), [5](#), [9](#)
- [21] M. F. Glasser, T. S. Coalson, E. C. Robinson, C. D. Hacker, J. Harwell, E. Yacoub, K. Ugurbil, J. Andersson, C. F. Beckmann, M. Jenkinson, and et al. A multi-modal parcellation of human cerebral cortex. *Nature*, 536(7615):171–178, 2016. [13](#), [15](#)
- [22] A. Gramfort, M. Luessi, E. Larson, D. A. Engemann, D. Strohmeier, C. Brodbeck, R. Goj, M. Jas, T. Brooks, L. Parkkonen, and M. S. Hämäläinen. MEG and EEG data analysis with MNE-Python. *Frontiers in Neuroscience*, 7(267):1–13, 2013. [8](#)
- [23] R. Grech, T. Cassar, J. Muscat, K. P. Camilleri, S. G. Fabri, M. Zervakis, P. Xanthopoulos, V. Sakkalis, and B. Vanrumste. Review on solving the inverse problem in eeg source analysis. *Journal of Neuro-Engineering and Rehabilitation*, 5(1), 2008. [9](#)

- [24] U. Hasson and C. J. Honey. Future trends in neuroimaging: Neural processes as expressed within real-life contexts. *NeuroImage*, 62(2):1272–1278, 2012. [4](#)
- [25] U. Hasson, O. Landesman, B. Knappmeyer, I. Vallines, N. Rubin, and D. Heeger. Neurocinematics: The neuroscience of film. *Projections*, 2:1–26, 06 2008. [3](#), [4](#)
- [26] M. A. Jatoi, N. Kamel, I. Faye, A. S. Malik, J. M. Bornot, and T. Begum. Bem based solution of forward problem for brain source estimation. *2015 IEEE International Conference on Signal and Image Processing Applications (ICSIPA)*, 2015. [10](#)
- [27] J. Josse and F. Husson. Selecting the number of components in principal component analysis using cross-validation approximations. *Computational Statistics Data Analysis*, 56(6):1869–1879, 2012. [14](#)
- [28] D. Kahneman. *Thinking, fast and slow*. Farrar, Straus and Giroux, 2013. [2](#)
- [29] Kauppi. Inter-subject correlation of brain hemodynamic responses during watching a movie: localization in space and frequency. *Frontiers in Neuroinformatics*, 2010. [6](#)
- [30] J. J. Ki, S. P. Kelly, and L. C. Parra. Attention strongly modulates reliability of neural responses to naturalistic narrative stimuli. *Journal of Neuroscience*, 36(10):3092–3101, 2016. [6](#)
- [31] N. Langer, E. J. Ho, L. M. Alexander, H. Y. Xu, R. K. Jozanovic, S. Henin, A. Petroni, S. Cohen, E. T. Marcelle, L. C. Parra, and et al. A resource for assessing information processing in the developing brain using eeg and eye tracking. *Scientific Data*, 4(1), 2017. [8](#), [9](#)
- [32] B. Leiter. Correlation is *not* causation pic.twitter.com/getzgk0l6, Oct 2021. [33](#)
- [33] Y. Lerner, K. S. Scherf, M. Katkov, U. Hasson, and M. Behrmann. Changes in cortical coherence supporting complex visual and social processing in adolescence. *Journal of Cognitive Neuroscience*, 33(11):2215–2230, 2021. [4](#)
- [34] G. Lioi, V. Gripon, A. Brahim, F. Rousseau, and N. Farrugia. Gradients of connectivity as graph fourier bases of brain activity. *Network Neuroscience*, 5(2):322–336, 2021. [13](#)
- [35] K. Mahjoory, V. V. Nikulin, L. Botrel, K. Linkenkaer-Hansen, M. M. Fato, and S. Haufe. Consistency of eeg source localization and connectivity estimates. *NeuroImage*, 152:590–601, 2017. [9](#)
- [36] J. Murphy and A. R. Pell. *Putting the power of your subconscious mind to work: reach new levels of career success using the power of your subconscious mind*. Prentice Hall Press, 2009. [22](#)
- [37] L. Naci, R. Cusack, M. Anello, and A. M. Owen. A common neural code for similar conscious experiences in different individuals. *Pro-*

- ceedings of the National Academy of Sciences*, 111(39):14277–14282, 2014. 6
- [38] M. Nentwich, L. Ai, J. Madsen, Q. K. Telesford, S. Haufe, M. P. Milham, and L. C. Parra. Functional connectivity of eeg is subject-specific, associated with phenotype, and different from fmri. *NeuroImage*, 218:117001, 2020. 8
 - [39] P. L. Nunez and R. Srinivasan. *Electric fields of the brain: the neuro-physics of EEG*. Oxford Univ. Pr., 2006. 2
 - [40] A. Ortega, P. Frossard, J. Kovacevic, J. M. F. Moura, and P. Vандергейст. Graph signal processing: Overview, challenges, and applications. *Proceedings of the IEEE*, 106(5):808–828, 2018. 6
 - [41] R. D. Pascual-Marqui, D. Lehmann, M. Koukkou, K. Kochi, P. Anderer, B. Saletu, H. Tanaka, K. Hirata, E. R. John, L. Prichep, and et al. Assessing interactions in the brain with exact low-resolution electromagnetic tomography. *Philosophical Transactions of the Royal Society A: Mathematical, Physical and Engineering Sciences*, 369(1952):3768–3784, 2011. 10
 - [42] R. A. Poldrack. *The new mind readers: what neuroimaging can and cannot reveal about our thoughts*. Princeton University Press, 2020. 4
 - [43] M. G. Preti and D. V. D. Ville. Decoupling of brain function from structure reveals regional behavioral specialization in humans. *Nature Communications*, 10(1), 2019. 13, 15
 - [44] J. Rué-Queralt, K. Glomb, D. Pascucci, S. Tourbier, M. Carboni, S. Vulliémoz, G. Plomp, and P. Hagmann. The connectome spectrum as a canonical basis for a sparse representation of fast brain activity. *NeuroImage*, 244:118611, 2021. 5, 6, 16
 - [45] A. K. Seth. *Being you: a new science of consciousness*. Dutton, an imprint of Penguin Random house LLC, 2021. 6
 - [46] J. Stiso and D. S. Bassett. Spatial embedding imposes constraints on neuronal network architectures. *Trends in Cognitive Sciences*, 22(12):1127–1142, 2018. 13
 - [47] F. Travis, D. A. F. Haaga, J. Hagelin, M. Tanner, A. Arenander, S. Nidich, C. Gaylord-King, S. Grosswald, M. Rainforth, R. H. Schneider, and et al. A self-referential default brain state: patterns of coherence, power, and eloreta sources during eyes-closed rest and transcendental meditation practice. *Cognitive Processing*, 11(1):21–30, 2009. 10
 - [48] UpAndRunning. Connectome - homepage. 13
 - [49] Y. Wang and Y. Wang. A neurocinematic study of the suspense effects in hitchcocks psycho. *Frontiers in Communication*, 5, 2020. 6
 - [50] J. Zaki and K. Ochsner. The need for a cognitive neuroscience of naturalistic social cognition. *Annals of the New York Academy of Sciences*, 1167(1):16–30, 2009. 4

- [51] J. Zhang, K. Chen, D. Wang, F. Gao, Y. Zheng, and M. Yang. Editorial: Advances of neuroimaging and data analysis. *Frontiers in Neurology*, 11, 2020. [4](#)

”Correlation is **not** causation”



Figure A.1: Meanwhile on twitter[32]